Volume 48 http://acousticalsociety.org/

22nd International Symposium on Nonlinear Acoustics

Oxford, UK
4-8 July 2022

Physical Acoustics: Session 1- Physics

A helicoidal parametric antenna for subwavelength vortex generation

Noé Jiménez
CSIC / Instituto de Instrumentación para Imagen Molecular, Universitat Politecnica de Valencia, Valencia, 46022, SPAIN; nojigon@upv.es

Joao Ealo and Rubén Darío Muelas-Hurtado
School of Mechanical Engineering,Universidad del Valle, Cali, COLOMBIA; joao.ealo@correounivalle.edu.co; ruben.muelas@correounivalle.edu.co

Aroune Duclos and Vicent Romero-García
Laboratoire d'Acoustique de l'Université du Mans, CNRS UMR 6613, Le Mans Universite, Le Mans, FRANCE; aroune.duclos@univ-lemans.fr; vicente.romero@univ-lemans.fr

The natural diffraction of acoustic vortex beams results in vortices whose bright core is larger than the wavelength, limiting their use for practical applications such as long-range underwater communications. In this work, we synthesize a vortex beam of sub-wavelength size at a distance beyond Rayleigh diffraction length using the nonlinear mixing of two confocal, high-frequency and detuned vortex beams of different topological charges. A helicoidal focused acoustic source with two different curvatures is used to generate a pair of finite-amplitude vortex beams. A difference-frequency component emerges due to nonlinearity. By tuning the primary beams, a low-frequency beam of integer topological charge is observed, whose distance between magnitude maxima is about 18 times smaller than its wavelength at a distance about 3 times the Rayleigh diffraction length. Subwavelength vortices of arbitrary topological charge emerge due to the spatiotemporal interference of two primary vortex beams and due to the conservation of angular momentum during nonlinear wave-mixing. This mechanism opens new venues to design directive parametric antennas for vortex transceivers or particle manipulation systems at scales well below the diffraction limit.

Published by the Acoustical Society of America

© 2022 Acoustical Society of America. https://doi.org/10.1121/2.0001629

1. INTRODUCTION

Acoustic vortex beams are structured wavefronts that show phase dependence of the type $\exp(il\phi)$, with ϕ the azimuthal angle and l the topological charge, respectively. At the principal axis of the vortex beam the field exhibits a phase singularity, therefore, the field at the axis is null. These beams have found several practical applications, such as rotation and particle manipulation[1–7] ultrasound imaging,[8] elastography,[9] communication, encoding and multiplexing,[10–12] or therapeutical ultrasound.[13] Methods to synthesize these beams include active devices such as phased arrays,[14] helical radiating surfaces[15] or Archimedean,[16,17] Fresnel spiral diffraction gratings,[18] or acoustic holograms,[19] among others. Metamaterials have also been used to generate vortex beams by using flat and sub-wavelength structures.[20,21] However, in all these configurations the natural diffraction of the wavefront limits the size of the vortex. The minimum value is only reached for distances smaller than the Rayleigh diffraction length of the source due to the divergence of the beam, given by the relation between the geometry of the source and the wavelength. Recently, increasing attention has been paid to restoring the evanescent components of a field to overcome the diffraction limit either using metamaterials[22] or time-reversal techniques.[23] However, as these approaches rely on evanescent waves, their use is restricted to near-field distances.

In this work,[24] we synthesize a vortex beam of sub-wavelength size at a distance beyond Rayleigh diffraction length using the nonlinear mixing of two confocal, high-frequency and detuned vortex beams of different topological charges. We demonstrate the concept using the natural self-demodulation phenomenon in air. We generate a focused vortex beam of integer topological charge whose distance between magnitude maxima is about 18 times smaller than its wavelength at a distance about 2.8 times the Rayleigh diffraction length.

2. METHODS

A device was manufactured by disposing 10-mm diameter ultrasound emitters operating in air over two different helical surfaces as shown in Fig. 1. The helical profile of the n-th surface (with $n = 1, 2$) was designed to generate a focused beam at a focal point, $\mathbf{r}(\phi, r, z) = (0, 0, F)$, and, simultaneously, produce at this location a difference of time of flight equal to $\Delta t_n = l_n\phi/\omega_n$, where l_n is the topological charge of the n-th primary vortex beam, ω_n the angular frequency and ϕ the azimuthal coordinate. In particular, the first source, composed of the two internal concentric rings of transducers, see Fig. 1 (b), was excited with a sinusoidal pulse burst of $\omega_1/2\pi = 40$ kHz while the second one, composed of the two external concentric rings of transducers, was excited at $\omega_2/2\pi = 41$ kHz. The topological charges of the primary vortex beams, defined by the curvature of the helical surfaces, were set to $l_1 = 1$ and $l_2 = 2$. Source aperture was set to $2a = 110$ mm, with a the radius of the source, and the focal point was $F = 100$ mm. Thus, the Rayleigh distances for the primary vortex beams are around $\pi a^2/\lambda_1 \approx \pi a^2/\lambda_2 \approx 1.1$ m.

The generation of the two confocal primary vortex beams is based on a helical surface. The surface should produce the focusing of the acoustic waves at the focal point $\mathbf{r}(x, y, z) = \mathbf{r}(0, 0, F)$ and, simultaneously, a phase dislocation at this point. The time-of-flight at the focal spot should present an azimuthal dependence of the type

$$\Delta t_n(\phi) = \frac{l_n\phi}{\omega_n}, \tag{1}$$

where l_n is the topological charge and ω_n the angular frequency of the n-th vortex beam and the azimuthal angle. To guarantee such phase, we design a helical surface as shown in Fig. 1 (a). The surface design is constrained by the distance to the focal point, which must follow this relation

$$R_n(\phi) = F - \frac{l_n\lambda_n\phi}{2\pi}, \tag{2}$$

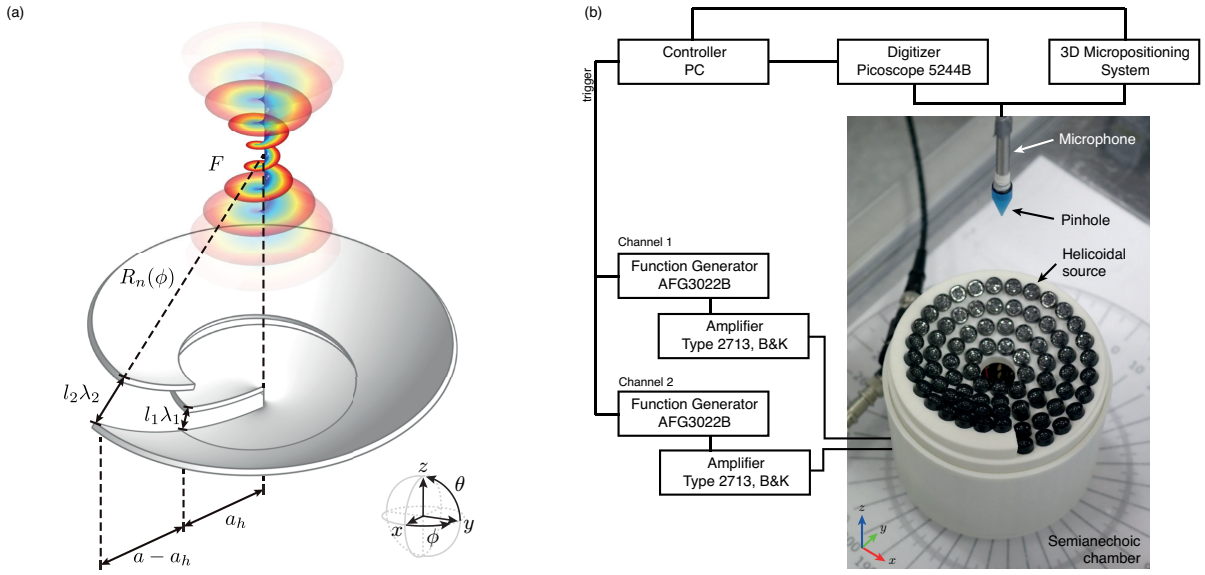


Figure 1: (a) Scheme of the helical surface to focus two confocal vortex beams. (b) Experimental setup.

at any point, where $\lambda_n = 2\pi c_0/\omega_n$. This surface, defined in spherical coordinates as $\mathbf{r} = \mathbf{r}(\phi, \theta, R_n(\phi))$, can be expressed in Cartesian coordinates as

$$x_n(\phi,\theta) = R_n(\phi)\cos(\phi)\sin(\theta), \tag{3}$$

$$y_n(\phi,\theta) = R_n(\phi)\sin(\phi)\sin(\theta), \tag{4}$$

$$z_n(\phi,\theta) = -\left[F + R_n(\phi)\cos(\theta)\right], \tag{5}$$

where the azimuthal and elevation angles range between $0 < \phi < 2\pi$ and $\theta^{[n]}_{\text{min}} < \theta < \theta^{[n]}_{\text{max}}$, respectively. The aperture angles are given by $\theta^{[2]}_{\text{max}} = \tan^{-1}(a/2F)$, $\theta^{[2]}_{\text{min}} = \tan^{-1}(a_h/2F)$, $\theta^{[1]}_{\text{max}} = \theta^{[2]}_{\text{min}}$, $\theta^{[1]}_{\text{min}} = 0$, where $2a$ is the outer-source aperture and $2a_h$is the aperture of the inner source.

The two vortex sources were manufactured by placing two concentric arrays of transducers over the helical surfaces. Each of the sources was composed of two concentric arrays of piezoelectric transducers, as shown in Fig. 1 (b). Each piezoelectric transducer (MA40S4S, Murata Manufacturing Co., Ltd.) presents an aperture of 10 mm and produces a sound pressure level of 120 dB SPL (0 dB = 20 μPa) measured at 30 cm in air when excited with a sinusoidal signal of 10 V. The source consisted in a total of 74 transducers (50 for the inner and 24 for the outer source). Transducers were connected in parallel. For the first source (inner array) the design frequency was $f_1 = 40$ kHz while for the second one (outer array) the frequency was $f_2 = 41$ kHz. The topological charges of the primary vortex beams were set to $l_1 = 1$ and $l_2 = 2$. Source aperture was $2a = 110$ mm ($2a_h = 60$mm) and the focal was $F = 100$ mm.

3. RESULTS

For finite-amplitude waves, and when all emitters are active, both beams interact and due to material and advective nonlinearity wave mixing occurs during propagation. Higher harmonics arise as arithmetical combinations of the fundamental waves of both beams. The root-mean-square pressure measured was 138.4 Pa at 40 kHz (a sound pressure level of 136.8 dB referenced at 20 μPa), enough to trigger weak nonlinear effects. In addition to higher harmonics, a difference-frequency mode of frequency $\omega_d = \omega_2 - \omega_1$ was generated due to the nonlinear self-demodulation of the beating wavefront.

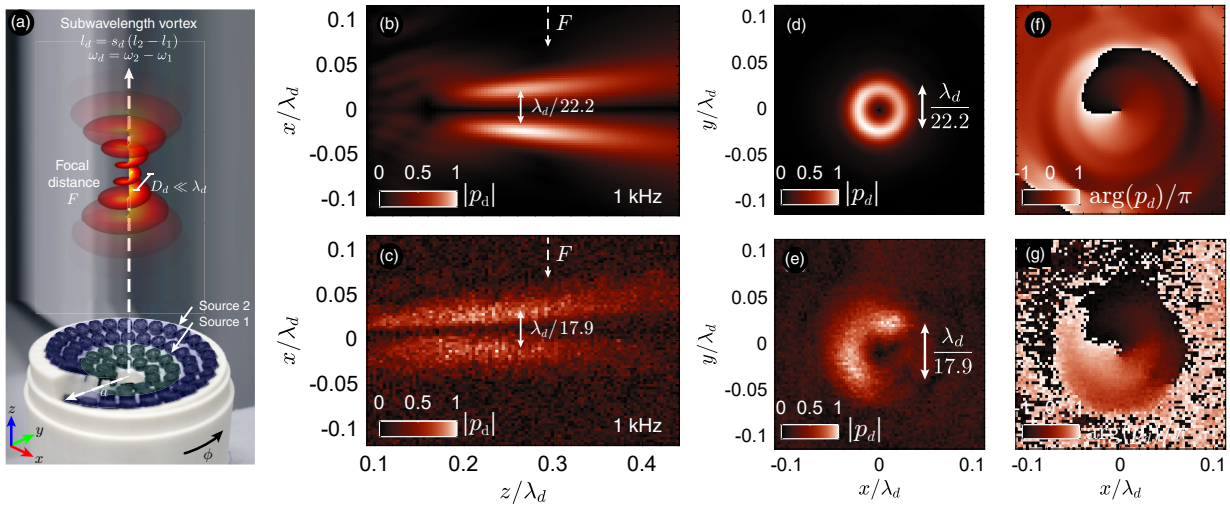


Figure 2: (a) scheme of the self-demodulated field. (b) and (c) show the sagittal field cross-sections at $y = 0$ ***showing the theoretical and measured demodulated component, respectively. (d-f) Transverse field cross-section at*** $z = 80$ ***mm showing the normalized magnitude (d,e) and the normalized phase (f,g) of the simulated and measured demodulated component, respectively.***

On the one hand, it is expected that the locally generated self-demodulated mode presents a field spatial distribution similar to those of the primary beams, as occurs in parametric acoustic antennas.[25] On the other hand, the phase of the self-demodulated beam depends on the spatiotemporal interference of the two vortex beams, which is linked to their topological charges. This results in a self-demodulated beam with a phase factor $\exp(il_d\phi)$ where the topological charge of the self-demodulated beam is

$$l_d = s_d(l_2 - l_1), \tag{6}$$

where $s_d = \text{sign}(\omega_2 - \omega_1)$, due to the conservation of topological charge of nonlinear vortices, which is indeed a consequence of the conservation of angular momentum.[26] Particular attention should be paid to Eq. (6) because this is not valid if the frequencies of the primary beams are commensurable.[27] However, in self-demodulation applications, this is usually fulfilled as the primary beams are commonly chosen with nearby frequencies. Therefore, to synthesize a sub-wavelength vortex by self-demodulation, the primary beams should present different topological charges and frequencies, and, in addition, their field distribution must overlap in space. Simulated and experimental results are shown in Fig. 2. A low-frequency beam at $\omega_d = 1$ kHz is generated locally, and its spatial distribution matches the overlapping volume of the two primary beams. Its corresponding wavelength is $\lambda_d = 2\pi c_0/\omega_d \gg \lambda_n$, therefore, the width of the beam, dominated by the width of the primary beams, is deep sub-wavelength.

The self-demodulated vortex arises as a result of the nonlinear mixing of the two primary vortex beams. Its topological charge is given by $l_d = l_2 - l_1 = 1$, showing the conservation of topological charge and, therefore, the conservation of orbital angular momentum during the nonlinear mixing of the primary beams as given by Eq. (6). The transversal pressure-field distribution of the self-demodulated vortex beam at $z = 80$ mm and $y = 0$ mm. The width of the vortex, D_d, is 17.9 times smaller than the wavelength in the experimental observations ($D_d = \lambda_d/22.2$ in simulations). Note that the measurement distance is 2.8 times the Rayleigh diffraction length for the self-demodulated mode. The field at the axis ($x = 0$) becomes null due to the phase singularity. The phase of the beam along the azimuthal coordinate ϕ, agrees with a linear profile of $(l_2 - l_1)\phi = l_d\phi$, demonstrating the topological charge conservation during nonlinear mixing. Using this approach, vortices of arbitrary topological charge and size can be synthesized by tuning the parameters of the primary beams.

4. CONCLUSIONS

In this work we have shown the sub-wavelength and sub-diffractive generation of acoustic vortices at distances beyond Rayleigh diffraction length by using the nonlinear self-demodulation. Sub-wavelength vortices emerge because of the spatiotemporal interference of two primary vortex beams due to the conservation of angular momentum during nonlinear wave-mixing. This mechanism can be used to transmit vortex-encoded information at larger distances. In this case, the topological charge of the self-demodulated vortex should be tuned using a reconfigurable emitter or a polar phased array system.

ACKNOWLEDGMENTS

We acknowledge financial support from the Spanish Ministry of Science, Innovation and Universities through grant "Juan de la Cierva – Incorporación" (IJC2018-037897-I) and PID2019-111436RB-C22, and by the Agència Valenciana de la Innovació through grants INNCON/2021/8 and INNVAL10/19/016, by Generalitat Valenciana through grant AICO/2020/268. Action co-financed by the European Union through the Programa Operativo del Fondo Europeo de Desarrollo Regional (FEDER) of the Comunitat Valenciana 2014-2020 (IDIFEDER/2018/022) and (IDIFEDER/2021/004). This article is based upon work from COST Action DENORMS CA15125. JPG and VRG gratefully acknowledge projects ANR-RGC METARoom (ANR-18-CE08-0021) and the HYPERMETA funded under the program Étoiles Montantes of the Région Pays de la Loire.

REFERENCES

[1] A. Anhäuser, R. Wunenburger, and E. Brasselet, "Acoustic rotational manipulation using orbital angular momentum transfer," *Phys. Rev. Lett.*, vol. 109, no. 3, p. 034301, 2012.

[2] D. Baresch, J.-L. Thomas, and R. Marchiano, "Observation of a single-beam gradient force acoustical trap for elastic particles: acoustical tweezers," *Phys. Rev. Lett.*, vol. 116, no. 2, p. 024301, 2016.

[3] A. Marzo, M. Caleap, and B. W. Drinkwater, "Acoustic virtual vortices with tunable orbital angular momentum for trapping of Mie particles," *Phys. Rev. Lett.*, vol. 120, no. 4, p. 044301, 2018.

[4] D. Baresch and V. Garbin, "Acoustic trapping of microbubbles in complex environments and controlled payload release," *Proc. Natl. Acad. Sci. U.S.A.*, vol. 117, no. 27, pp. 15490–15496, 2020.

[5] M. Baudoin, J.-C. Gerbedoen, A. Riaud, O. B. Matar, N. Smagin, and J.-L. Thomas, "Folding a focalized acoustical vortex on a flat holographic transducer: miniaturized selective acoustical tweezers," *Sci. Adv.*, vol. 5, no. 4, p. eaav1967, 2019.

[6] M. Baudoin, J.-L. Thomas, R. Al Sahely, J.-C. Gerbedoen, Z. Gong, A. Sivery, O. B. Matar, N. Smagin, P. Favreau, and A. Vlandas, "Spatially selective manipulation of cells with single-beam acoustical tweezers," *Nat. Commun.*, vol. 11, no. 1, pp. 1–10, 2020.

[7] M. A. Ghanem, A. D. Maxwell, Y.-N. Wang, B. W. Cunitz, V. A. Khokhlova, O. A. Sapozhnikov, and M. R. Bailey, "Noninvasive acoustic manipulation of objects in a living body," *Proc. Natl. Acad. Sci. U.S.A.*, 2020.

[8] T. Brunet, J.-L. Thomas, and R. Marchiano, "Transverse shift of helical beams and subdiffraction imaging," *Physical review letters*, vol. 105, no. 3, p. 034301, 2010.

[9] N. Jiménez, J. M. Benlloch, and F. Camarena, "A new elastographic technique using acoustic vortices," in *2020 IEEE International Ultrasonics Symposium (IUS)*, pp. 1–4, IEEE, 2020.

[10] C. Shi, M. Dubois, Y. Wang, and X. Zhang, "High-speed acoustic communication by multiplexing orbital angular momentum," *Proc. Natl. Acad. Sci. U.S.A.*, vol. 114, no. 28, pp. 7250–7253, 2017.

[11] X. Jiang, B. Liang, J.-C. Cheng, and C.-W. Qiu, "Twisted acoustics: metasurface-enabled multiplexing and demultiplexing," *Advanced Materials*, vol. 30, no. 18, p. 1800257, 2018.

[12] X. Jiang, C. Shi, Y. Wang, J. Smalley, J. Cheng, and X. Zhang, "Nonresonant metasurface for fast decoding in acoustic communications," *Physical Review Applied*, vol. 13, no. 1, p. 014014, 2020.

[13] S. Jiménez-Gambín, N. Jiménez, and F. Camarena, "Transcranial focusing of ultrasonic vortices by acoustic holograms," *Physical Review Applied*, vol. 14, no. 5, p. 054070, 2020.

[14] B. T. Hefner and P. L. Marston, "An acoustical helicoidal wave transducer with applications for the alignment of ultrasonic and underwater systems," *Jour. Acous. Soc. Am.*, vol. 106, no. 6, pp. 3313–3316, 1999.

[15] J. L. Ealo, J. C. Prieto, and F. Seco, "Airborne ultrasonic vortex generation using flexible ferroelectrets," *IEEE Trans. Ultrason. Ferroelectr. Freq. Control*, vol. 58, no. 8, pp. 1651–1657, 2011.

[16] N. Jiménez, V. Sánchez-Morcillo, R. Picó, L. Garcia-Raffi, V. Romero-Garcia, and K. Staliunas, "High-order acoustic bessel beam generation by spiral gratings," *Physics Procedia*, vol. 70, pp. 245–248, 2015.

[17] N. Jiménez, R. Picó, V. Sánchez-Morcillo, V. Romero-García, L. M. García-Raffi, and K. Staliunas, "Formation of high-order acoustic Bessel beams by spiral diffraction gratings," *Phys. Rev. E*, vol. 94, no. 5, p. 053004, 2016.

[18] N. Jiménez, V. Romero-García, L. M. García-Raffi, F. Camarena, and K. Staliunas, "Sharp acoustic vortex focusing by Fresnel-spiral zone plates," *Appl. Phys. Lett.*, vol. 112, no. 20, p. 204101, 2018.

[19] S. Jiménez-Gambín, N. Jiménez, J. M. Benlloch, and F. Camarena, "Generating bessel beams with broad depth-of-field by using phase-only acoustic holograms," *Sci. Rep.*, vol. 9, no. 1, pp. 1–13, 2019.

[20] X. Jiang, Y. Li, B. Liang, J.-c. Cheng, and L. Zhang, "Convert acoustic resonances to orbital angular momentum," *Phys. Rev. Lett.*, vol. 117, no. 3, p. 034301, 2016.

[21] A. Marzo, A. Ghobrial, L. Cox, M. Caleap, A. Croxford, and B. Drinkwater, "Realization of compact tractor beams using acoustic delay-lines," *Appl. Phys. Lett.*, vol. 110, no. 1, p. 014102, 2017.

[22] J. B. Pendry, "Negative refraction makes a perfect lens," *Phys. Rev. Lett.*, vol. 85, no. 18, p. 3966, 2000.

[23] G. Lerosey, J. De Rosny, A. Tourin, and M. Fink, "Focusing beyond the diffraction limit with far-field time reversal," *Science*, vol. 315, no. 5815, pp. 1120–1122, 2007.

[24] N. Jiménez, J. Ealo, R. D. Muelas-Hurtado, A. Duclos, and V. Romero-García, "Subwavelength acoustic vortex beams using self-demodulation," *Physical Review Applied*, vol. 15, no. 5, p. 054027, 2021.

[25] P. J. Westervelt, "Parametric acoustic array," *Jour. Acous. Soc. Am.*, vol. 35, no. 4, pp. 535–537, 1963.

[26] J.-L. Thomas and R. Marchiano, "Pseudo angular momentum and topological charge conservation for nonlinear acoustical vortices," *Phys. Rev. Lett.*, vol. 91, no. 24, p. 244302, 2003.

[27] R. Marchiano and J.-L. Thomas, "Doing arithmetic with nonlinear acoustic vortices," *Physical review letters*, vol. 101, no. 6, p. 064301, 2008.